FEBS Letters 545 (2003) 224–228 FEBS 27342

pH dependence studies provide insight into the structure and mechanism of thimet oligopeptidase (EC 3.4.24.15)

Jeffrey A. Sigman[a], Sarah R. Edwards[a], Amanda Pabon[b], Marc J. Glucksman[b], Adele J. Wolfson[a,*]

[a] *Department of Chemistry, Wellesley College, Wellesley, MA 02481, USA*
[b] *FUHS/Chicago Medical School, Midwest Proteome Center, Chicago, IL, USA*

Received 17 March 2003; revised 12 May 2003; accepted 12 May 2003

First published online 23 May 2003

Edited by Hans Eklund

Abstract Thimet oligopeptidase (EC 3.4.24.15; TOP) is a Zn(II) endopeptidase implicated in physiological regulation of processes involving neuropeptides. The present study clarifies the active site structure and mechanism of catalysis of TOP. The enzyme exhibited a bell-shaped pH dependence of activity having an acidic limb due to a protonation event with a pK_a of 5.7 and a basic limb with pK_a of 8.8. The acidic limb can be attributed to protonation of a residue affecting k_{cat} while the alkaline limb may be due to conformational change. Mutation of Tyr612 to Phe resulted in more than 400-fold decrease in activity. This result, supported by modeling studies, implicates Tyr612 in transition state stabilization analogous to the role of His231 of thermolysin.

Key words: Homology modeling; Thimet oligopeptidase; Metal activation; pH dependence; Transition state stabilization; Tyrosine

1. Introduction

Thimet oligopeptidase (TOP) is a 78-kDa endopeptidase (EC 3.4.24.15) that hydrolyzes important neuropeptides including bradykinin, neurotensin, somatostatin, and gonadotropin-releasing hormone [1–6]. The primary sequence of TOP places it within the class of zinc metalloendopeptidases that includes neurolysin, neutral endopeptidase, and angiotensin-converting enzyme [7,8]. Of these, neurolysin is its closest homolog, sharing $>60\%$ sequence identity [9]. The active site of neurolysin also bears similarity to that of thermolysin especially in terms of Zn(II) coordination [10]. In thermolysin an active site residue, His231, has been proposed to stabilize the developing negative charge in the transition state by H-bond formation [11]. Based on the X-ray structure [10], Tyr613 in neurolysin (Tyr612 in TOP) occupies a similar position and is proposed to play a similar kinetic role.

In order to gain further insight into the mechanism of TOP and to establish the unique role of Tyr612, we have studied the activity of the wild-type TOP (WT TOP) and of a Tyr612-Phe variant as a function of pH. The experimental results are supported by homology modeling of TOP using neurolysin as the template structure. The model has been evaluated and the resulting structure used in conjunction with experiments to clarify the mechanism and active site structure of TOP.

2. Materials and methods

2.1. Materials

Glutathione Sepharose, Sephacryl S-200, and PD-10 columns were obtained from Amersham Pharmacia Biotech (Piscataway, NJ, USA). The 7-methoxycoumarin-4-acetyl-Pro-Leu-Gly-Pro-Lys-dinitrophenol (MCA) fluorescent substrate was obtained from Bachem (King of Prussia, PA, USA). All other reagents were purchased from Sigma Chemical Co (St. Louis, MO, USA).

2.2. Recombinant TOP

TOP (accession number P24155) was expressed and purified, and site-directed mutagenesis performed using the TOP expression vector, GEX-24.15 as previously described [12]. Prokaryotic codon usage rules were used to prevent the use of rare codons that may hinder expression of the mutant proteins. At least two independent preparations of WT protein and Tyr612Phe TOP were purified and characterized, with similar homogeneity, yields, and kinetic parameters. The enzyme concentration was determined using the molar extinction coefficient $\varepsilon_{280} = 73.11\ mM^{-1}\ cm^{-1}$, calculated based on the amino acid content of the protein using the automated ProtParam Tool on the SWISS ExPASy server [13]. In order to verify structural integrity of the recombinant proteins, far-ultraviolet circular dichroism (UV CD) and fluorescence analyses were carried out using an AVIV 60DS spectropolarimeter and Cary Eclipse spectrofluorimeter. Spectra of the mutated protein Tyr612Phe TOP normalized for protein concentration indicated no alterations in the net conformation of the mutant as compared to WT (data not shown).

2.3. Homology modeling

The three-dimensional structure of TOP was modeled to the fold of neurolysin using atomic coordinates (Protein Data Bank, 1I1I.pdb) from the recently determined X-ray crystal structure of neurolysin [10]. The initial model was generated in SWISS PDBviewer version 3.72 [14–16] using the program Magic-Fit in the viewer software suite and refined and evaluated both by visual inspection and using the software provided in SWISS PDBviewer version 3.72.

2.4. Kinetic assays

All kinetic assays were performed using a Cary Eclipse spectrofluorimeter. Cleavage of the fluorogenic MCA substrate [17] was monitored by the increase in emission at 400 nm over time using a λ_{ex} of 325 nm. Less than 10% of the substrate was consumed assuring first-order kinetics of the reaction. Assays were performed in duplicate at 37 and 25°C in 25 mM Bis–Tris, in 25 mM Tris, and in 25 mM CHES buffer with each adjusted to a conductivity of 15 mS/cm^2 with

*Corresponding author. Fax: (1)-781-283 3642.
E-mail address: awolfson@wellesley.edu (A.J. Wolfson).

Abbreviations: TOP, thimet oligopeptidase; MCA, 7-methoxycoumarin-4-acetyl-Pro-Leu-Gly-Pro-Lys-dinitrophenol; DTT, dithiothreitol; cFP, *N*-[1-(*RS*)-carboxy-3-phenylpropyl]-Ala-Ala-Tyr-p-aminobenzoate; CPA, carboxypeptidase A

0014-5793/03/$22.00
doi:10.1016/S0014-5793(03)00548-9

NaCl and containing 0.15 mM dithiothreitol (DTT). MCA substrate concentration was calculated based on the molar extinction coefficient ε_{365} (17.3 mM^{-1} cm^{-1}) of the 2,4-dinitrophenol. The change in fluorescence intensity over time was converted to rate of product formation using a standard curve calculated for the peptide product, 7-methoxycoumarin-4-acetyl-Pro-Leu-OH. Additional measures were taken to insure that the observed changes in activity over the experimental pH range were due to protonation events in the active site and not artifacts of protein denaturation or loss of Zn(II). First, to rule out any change due to denaturation, the activity of the protein incubated and assayed at pH 7.3 was compared to protein that was incubated at the pH extremes for 10–15 min and then assayed at pH 7.3 (data not shown). No difference in the protein activity was observed under these conditions. Second, all activity assays were performed in the presence of 1 μM Zn(II) added to the buffer.

The pseudo-first-order rate constant, k, of enzyme activity was determined under conditions in which $[E] \ll [S] \ll K_m$ and calculated from the slope of the linear least squares fit to the graph of initial substrate concentration (μM) vs. rate of product formation (μM/s). Each plot was defined by four to five points and had an r^2 value of at least 0.99. The kinetic parameters, V_{max} and K_m, were determined using a hyperbolic fit (rate = $V_{max}[S]/(K_m+[S])$) to the plot of substrate concentration (μM) vs. rate of product formation (μM/s) and by Eadie–Hofstee plots under conditions in which [S] is above and below K_m. Analysis of the pH dependence of the kinetic parameters was done by a non-linear least squares fit of the data points to Eqs. 1 and 2. All fitting procedures were performed using the program T-curve (SPSS Inc).

2.5. Intrinsic fluorescence

Intrinsic (Trp) fluorescence of both WT and Tyr612Phe TOP was measured in 25 mM Tris buffers, at pH values from 7.2 to 9.6, conductivity 15 mS/cm^2, containing DTT. Fluorescence was monitored at 25°C for each sample, λ_{ex} = 280 nm, emission from 300 to 475 nm. Protein concentration was 0.6 μM for WT and 1.0 μM for Tyr612Phe TOP.

3. Results

3.1. Activity of the Tyr612Phe mutant

Summarized in Table 1 are the resulting kinetic parameters, k_{cat}, K_m, and k_{cat}/K_m, derived from Michaelis–Menten plots for cleavage of the MCA substrate by WT TOP and Tyr612Phe TOP at pH 7.8 in Tris buffer with 10 mM $CaCl_2$. The conservative change of removing the hydroxyl group from Tyr results in a 400-fold decrease in k_{cat}/K_m. Furthermore, this change is entirely due to a decrease in catalytic rate. The apparent binding of the substrate is only marginally affected by the mutation, while k_{cat} decreases by greater than 350-fold.

To illustrate further that the effect of the Tyr to Phe mutation is catalytic and not structural, we determined the effect of the mutation on the binding of the TOP-specific inhibitor, *N*-[1-(*RS*)-carboxy-3-phenylpropyl]-Ala-Ala-Tyr-p-aminobenzoate (cFP). The resulting K_I values, determined over a 10-fold range in inhibitor concentration, are listed in Table 1. The affinity for cFP decreases by only 2-fold as a result of the mutation.

3.2. Dependence of the kinetic parameters on pH

Enzymatic activity was determined as a function of pH. Shown in Fig. 1a is the pH dependence of k_{cat}/K_m for TOP activity over a pH range from 5.2 to 9.5 in 25 mM Bis–Tris or Tris buffer. The curve is bell-shaped, as has been observed for other classes of metallopeptidases [18–21] with a plateau in activity between pH 6.5 and 8. Curve fitting of the data to the equation

$$k_{app} = \frac{k_{lim}}{1 + 10^{pK_{a\ acidic} - pH} + 10^{pH - pK_{a\ alkaline}}} \quad (1)$$

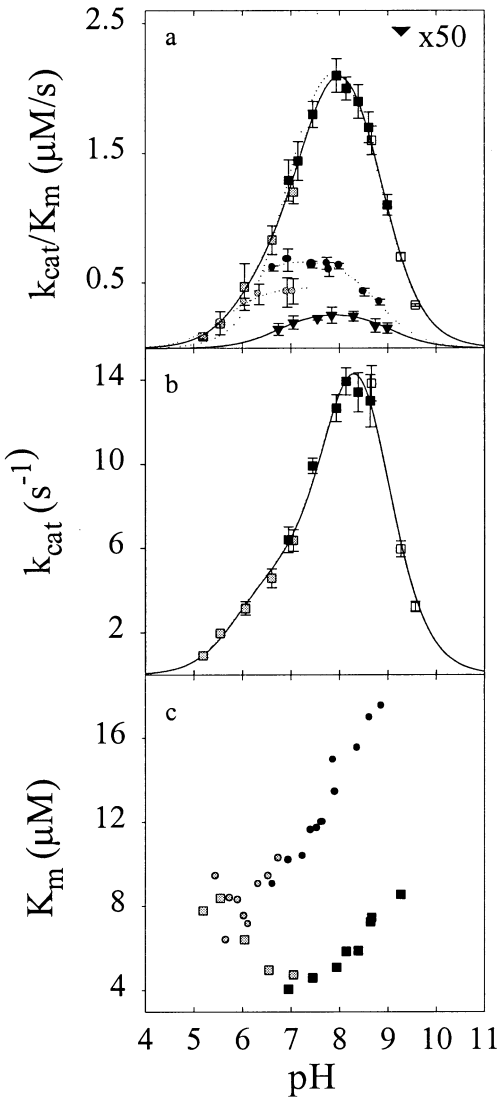

Fig. 1. pH dependence of the kinetic parameters for MCA hydrolysis by TOP. Shown are the pH-dependent changes in a: k_{cat}/K_m, b: k_{cat}, and c: K_m for WT TOP (circles), WT TOP with 10 mM $CaCl_2$ (squares), and Tyr612Phe TOP (triangles). Activity assays were carried out in 25 mM Bis–Tris buffer (gray filled); 25 mM Tris buffer (black filled), and 25 mM CHES (open), all containing 0.15 mM DTT and with conductivity of 15 mS/cm^2. The dotted lines represent the non-linear least squares fit of the data to Eq. 1. Solid lines represent the non-linear least squares fit of the data to Eq. 2. The pK_a values derived for the ionization of groups limiting in catalysis are listed in Table 2.

Table 1
Kinetic parameters of WT TOP and Y612F TOP at pH 7.8

Protein	k_{cat}/K_m (μM^{-1} s^{-1})	k_{cat} (s^{-1})	K_m (μM)	K_I cFP (nM)
WT TOP	2.2 ± 0.1	9.9 ± 0.4	4.6 ± 0.4	14.2 ± 0.1
Y612F	0.0053 ± 0.0001	0.027 ± 0.002	5.1 ± 0.5	29.8 ± 0.3

in which k_{lim} is the limiting kinetic parameter, yielded the pK_a values (Table 2) for the residues responsible for the acidic and alkaline limbs of the curve. The acidic limb occurs at p$K_{a\ acidic} = 5.7$ which is similar to those for thermolysin and carboxypeptidase A (CPA) [19,20]. The alkaline limb occurs at p$K_{a\ alkaline} = 8.8$. This is distinct from that of thermolysin (p$K_a = 8.0$) but closer to that of CPA (p$K_a = 9.0$) [18,21]. A similar profile was obtained for WT TOP at 25°C. Although the values of kinetic parameters varied with temperature, the pK_a value corresponding to the alkaline limb under this set of conditions was 9.3 ± 0.7 (data not shown).

The plots of pH vs. k_{cat}/K_m for the Tyr612 mutant and WT TOP, both in the presence of 10 mM $CaCl_2$, are shown in Fig. 1a and summarized in Table 2. Previous studies indicated that activity of TOP with the MCA substrate is enhanced at least 2-fold by the addition of $CaCl_2$ in the reaction buffer [17]. Since the activity of the mutant is significantly less than that of the WT TOP, $CaCl_2$ was included in the reaction buffer. The mutant and WT exhibited similar decreases in the acidic and alkaline limbs, and with the addition of 10 mM $CaCl_2$, the acidic limb of the WT enzyme shifted. Below pH 6.5, the determined rate constants deviate from the least squares fit line obtained using Eq. 1 (Fig. 1a, dotted line). Better results were obtained if three ionizations were considered using the equation

$$k_{app} = \frac{k_{lim1} + k_{lim2}10^{pH-pK_{a\ acidic2}}}{1 + 10^{pK_{a\ acidic1}-pH} + 10^{pH-pK_{a\ acidic2}}(1 + 10^{pH-pK_{a\ alkaline}})} \quad (2)$$

in which k_{lim1} and k_{lim2} are the limiting kinetic parameters for the first (p$K_{a\ acidic1}$) and second (p$K_{a\ acidic2}$) ionization steps. The resulting curve, shown as a solid line in Fig. 2, yields pK_a values of 5.9, 7.3, and 8.9 as summarized in Table 2.

The dependence of the individual kinetic constants K_m and k_{cat} with respect to pH was also examined (Fig. 1b and c). The results demonstrate that as pH is increased, both K_m and k_{cat} increase. This finding is consistent with a bell-shaped kinetic profile, since at low pH binding is tighter but k_{cat} is smaller, and conversely at higher pH k_{cat} is increased but the substrate affinity becomes weaker. Fig. 1b shows that k_{cat} increases with increasing pH to a plateau between pH 8.5 and 9.0. Similar to the trend observed for k_{cat}/K_m over the same pH range, the acidic limb of the data can be fitted to a single ionization step only if the points below pH 6.5 are disregarded. A better fit to the data is obtained if two pK_a values are considered in the acidic limb using Eq. 2. This yields pK_a values of 5.8, 7.9 and 8.9 as listed in Table 2. These match well to the pK_a values determined for the pH vs. k_{cat}/K_m profiles without (p$K_a = 5.7$ and 8.8) and with calcium (p$K_a = 5.9$, 7.3, 8.9).

The pH dependence of K_m when $CaCl_2$ is used in the buffer differs significantly from that observed without calcium. Fig. 1c shows that calcium increases the affinity of TOP for the MCA substrate, resulting in a better than 2-fold decrease in K_m over the pH range from 7 to above 9. However, proceeding from pH 7 to 5, K_m begins to rise back to the level without calcium. For instance, at pH 7.0 the K_m with calcium is 4 μM compared to ~10 μM without. At pH 5.8 however, K_m under both conditions is ~10 μM.

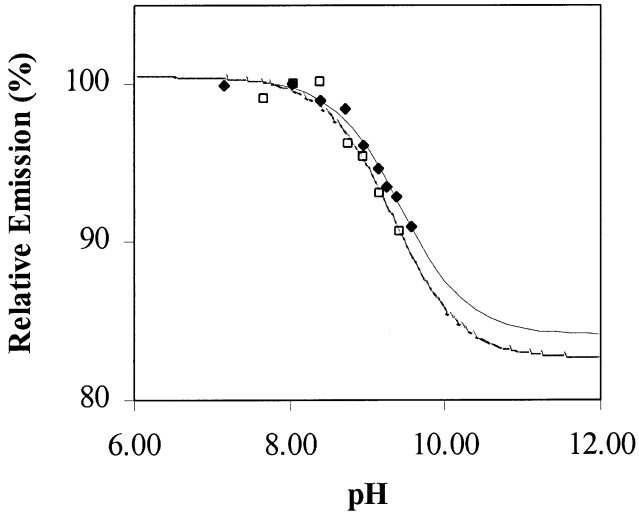

Fig. 2. Intrinsic fluorescence change of WT (closed diamonds) and Tyr612Phe (open squares) TOP as a function of pH. Solid lines represent the fit of the data points to a sigmoidal function. Data were normalized to known fluorescence intensity at pH 8.0.

3.3. Effect of pH on intrinsic fluorescence

Fig. 2 contains the results of Trp fluorescence of the WT and Tyr162Phe mutant enzymes from pH 7.8 to 9.6. Both forms of the enzyme displayed a decrease in fluorescence intensity at high pH. The pK_a of the decline for WT was 9.4 ± 0.1, and for the mutant was 9.3 ± 0.3.

4. Discussion

Though much biochemical data have been reported for TOP, very little evidence has been gathered about the structure of the protein. A detailed study comparing the crystal structure of neurolysin [10], a homolog of TOP sharing >60% sequence identity and nearly 80% sequence similarity to TOP, has recently been published [22]; however, that work focused mainly on substrate recognition rather than catalytic mechanism. In the present study, a molecular model of the TOP active site has been generated to aid in the analysis of the experimental results. A diagram of the active site of TOP

Table 2
pH dependence of kinetic parameters

	Ca^{2+}	Equation	p$K_{a\ acidic1}$	p$K_{a\ acidic2}$	p$K_{a\ alkaline}$
WT TOP					
k_{cat}/K_m	−	1	5.7 ± 0.2		8.8 ± 0.2
k_{cat}/K_m[a]	+	1		6.9 ± 0.3	8.9 ± 0.2
$k_{cat}K_m$	+	2	5.9 ± 0.6	7.3 ± 0.3	8.9 ± 0.1
k_{cat}	+	2	5.8 ± 0.5	7.9 ± 0.4	8.9 ± 0.2
Y612F TOP					
k_{cat}/K_m[a]	+	1		6.7 ± 0.3	9.0 ± 0.2

[a]Fit in pH range 6.5–9.6.

as modeled is shown in Fig. 3 overlaid onto the active site of thermolysin determined by X-ray diffraction [23]. Despite the lack of sequence homology between thermolysin and TOP there is a striking conservation predicted in their secondary, and hence tertiary structures, especially in their active sites.

The pH dependence of TOP activity supports an active site structure as shown in Fig. 3. The bell-shaped pH profile of k_{cat}/K_m shown in Fig. 1a is similar to those obtained for thermolysin and CPA [18–21]. The acidic limb in Fig. 1a indicates that a residue with a pK_a of 5.7 is important for catalysis (see Table 2). The same pH dependence is observed in thermolysin and CPA (pK_{a1} = 5.3 and 6.0, respectively) and this ionization is usually assigned to the Glu in the HisGluXaaXaaHis motif (analogous to Glu474 in TOP) [24]. Based on the crystal structure of thermolysin bound to several inhibitors, this Glu residue is believed to accept an H-bond from the water nucleophile and then transfer the proton to the leaving amine [11]. Protonation of this residue (or the Glu-water unit) as the pH is lowered results in a decrease in k_{cat} [20]. The results in Fig. 1a,b definitively show that the acidic limb of the pH vs. k_{cat}/K_m profile is associated with a residue affecting k_{cat}. The first ionization at pH 5.7 in the plots of pH vs. k_{cat}/K_m, under both sets of conditions (i.e. with and without $CaCl_2$) appears in the pH dependence of k_{cat}. This ionization can thus be assigned to a Glu474-water unit in TOP. This result adds additional evidence that a Glu residue is the third Zn(II) ligand since a $His_3Zn(II)OH_2$ coordination sphere would exhibit an elevated pK_a for the Glu-water unit in the acidic limb.

The second ionization (see Table 2) observed in the acidic limb of the k_{cat}/K_m and k_{cat} profiles with $CaCl_2$ present in the buffer is more difficult to assign. Though calcium increases the affinity of TOP for the MCA substrate [17], this could be an electrostatic effect neutralizing the net charge on the protein and allowing more efficient binding of the very non-polar MCA substrate. However, with the pH dependence of k_{cat}, calcium must be playing an additional role. As seen in Fig. 1b, calcium has the greatest effect on k_{cat} at pH levels above 8, but this effect drops off due to the protonation of a group with a pK_a between 7 and 8. For this reason it seems unlikely that it is due to the protonation of a protein-based ligand to Ca(II), since these would be oxyanion based and not likely have pK_a's within this range. Therefore, a calcium-bound water may be participating in the transfer of protons during the reaction. At high pH the deprotonated water bound to calcium is able to accept protons during the reaction mechanism. As the pH falls below 8, this calcium-bound hydroxide becomes protonated and can no longer participate in the mechanism, but may enhance ligand binding. As the pH falls below 6.5, K_m rises to the value observed without calcium, ~10 μM (Fig. 1c). Thus, as shown in Fig. 1a, k_{cat}/K_m is identical with or without calcium at pH 5.3. Further study is needed to determine the exact role and number of calcium ions involved in enhancing the activity of TOP towards the MCA substrate.

A definitive structure–function role is now established for Tyr612 in the mechanism of TOP. The model predicts that the side chain oxygen of Tyr612 is within 5.4 Å of the active site Zn(II). Based on X-ray crystallography, a role in substrate binding and transition state stabilization has been proposed for the equivalent Tyr residue in neurolysin and also more recently in a thermostable carboxypeptidase [25], although no kinetic evidence has yet been presented to support that role. Tyr612 is in a similar position with respect to the active site as His231 in thermolysin [10], displaying the alternate position of the zinc-bound water (Fig. 3) [11,23]. In thermolysin, the tetrahedral transition state intermediate formed at the carbonyl carbon of the scissile peptide bond is stabilized by an H-bond from His231. In the thermolysin-like enzyme from *Bacillus stearothermophillus*, mutation of this residue to Phe leads to a 430- to 500-fold decrease in k_{cat}/K_m and removes the pH dependence in the alkaline limb of the enzyme's pH vs. k_{cat}/K_m profile, which normally occurs at pH 8.0 [26]. Likewise, an identical 400-fold drop in k_{cat}/K_m is associated with mutating Tyr612 to Phe in TOP. This leads to a $\Delta\Delta G$ for removal of the Tyr hydroxyl of 3.7 kcal/mol, identical to the value observed in thermolysin and similar enzymes [26,27].

The active site of thermolysin also contains a Tyr residue (Tyr157) that has been implicated in transition state stabilization, and substitution of Phe for this Tyr residue decreases activity approximately 200-fold [28] compared to the 500 times reduction in activity with His231 mutants [26]. Both

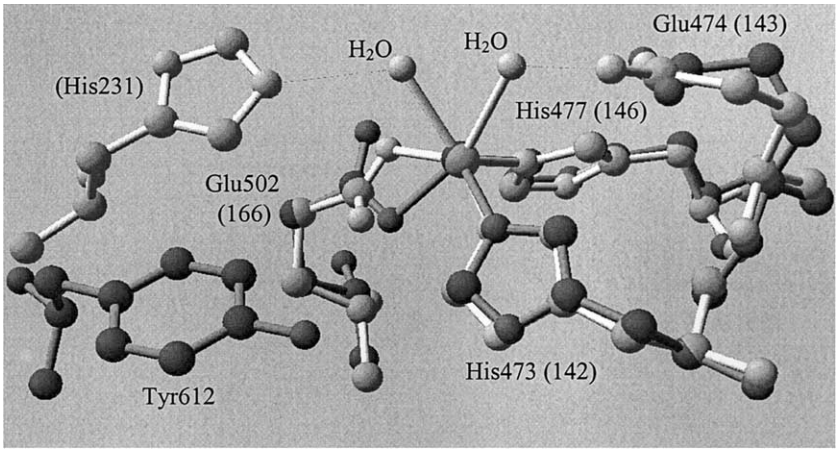

Fig. 3. Comparison of the active sites of thermolysin (light gray) and TOP model (dark gray). Shown are the three protein-based Zn(II) ligands, two water molecules present in the X-ray crystal structure of thermolysin, the Glu residues proposed to be involved in crucial H-bond interactions with the nucleophilic water, and Tyr612 and His231, the residues proposed to stabilize the developing negative charge in the transition state by H-bond donation [11,23]. Residue numbers for thermolysin are shown in parentheses.

Tyr157 and His231 may be involved in transition state stabilization. However, Tyr157 lies on the opposite side of the transition state intermediate in comparison to His231 (and Tyr612 in TOP). His231 of thermolysin is conserved in the primary structure of both TOP and neurolysin but not in the tertiary structure of neurolysin [10] (or as modeled for TOP). However, the position, geometry, and loss in activity upon mutation of Tyr612 of TOP are comparable to those of His231 in thermolysin, strongly suggesting that Tyr612 plays a similar mechanistic role in peptide hydrolysis by donating a hydrogen bond to the transition state intermediate.

Because of the involvement of both His and Tyr residues in thermolysin, another related metalloprotease, astacin, may represent a better model for the role of Tyr in TOP's active site [10]. In astacin, a single Tyr residue (Tyr149) is thought to stabilize the transition state [29], donating a hydrogen bond as we propose for TOP. However, the situation for astacin is complicated by the fact that Tyr149 acts as a fifth ligand for the active site zinc, and must undergo rearrangement before substrate binding and catalysis [30]. It is interesting to note that although Tyr has not been shown to be a Zn(II) ligand in neurolysin or TOP, based on the model presented here (Fig. 3), Tyr612 must undergo some reorganization upon substrate binding in order to perform its role in transition state stabilization.

In contrast to the situation for thermolysin, the alkaline limb in the pH dependence of k_{cat}/K_m is not lost upon removal of Tyr612. Both WT TOP and the Tyr612 mutant of TOP (Fig. 1) show a decrease in activity at high pH associated with a residue having a pK_a of 8.9. Thus, Tyr612 must have a normal pK_a of 10 which is outside of the pH range used in this study. This is consistent with the microenvironment of Tyr612: in the absence of substrate, the hydroxyl group of Tyr612 would be surrounded by solvent and not hydrogen bonded to other residues thereby lowering its pK_a. Fluorescence profiles (Fig. 2) suggest that the loss in activity at alkaline pH is due to a conformational change in the enzyme rather than a deprotonation event. The pK_a of the decline in fluorescence corresponds to the pK_a of the alkaline limb of the activity profile, and suggests a basis for the loss in activity.

In conclusion, this study represents kinetic evidence that the mechanism of peptide hydrolysis by TOP, a mammalian neuropeptide processing enzyme, is similar to that previously postulated for bacterial thermolysin-like enzymes. As with those enzymes, Glu474 of the HisGluXaaXaaHis motif serves to deprotonate the incoming water nucleophile. Upon attack by the nucleophile, the double bond of the peptide carbonyl breaks and a crucial amino acid in the active site is available to donate a hydrogen bond, thus stabilizing the developing negative charge on the C-terminal oxygen in the transition state. Furthermore, the identification of Tyr612 in TOP as the amino acid corresponding in function to the classic histidine in thermolysin-like enzymes clarifies the mechanism of this group of enzymes. Since submission of this work, a report has appeared demonstrating the effect of mutation of Tyr612 in TOP and Tyr613 in neurolysin [31].

Acknowledgements: This work was supported by a Howard Hughes Medical Institute Undergraduate Science Education Program Grant, a National Science Foundation Research Experiences for Undergraduates Award, the NIH/National Institute of Neurological Disorders and Stroke NS 39892 (M.J.G.), and by a Camille and Henry Dreyfus Scholar/Fellow Award.

References

[1] Camargo, A.C., Oliveira, E.B., Toffoletto, O., Metters, K.M. and Rossier, J. (1987) J. Neurochem. 48, 1258–1263.
[2] Camargo, A.C.M., Gomes, M.D., Reichl, A.P., Ferro, E.S., Jacchieri, S., Hirata, I.Y. and Julianos, L. (1997) Biochem. J. 324, 517–522.
[3] Dahms, P. and Mentlein, R. (1992) Eur. J. Biochem. 208, 145–154.
[4] Lew, R.A., Hey, N.J., Tetaz, T.J., Glucksman, M.J., Roberts, J.L. and Smith, A.I. (1995) Biochem. Biophys. Res. Commun. 209, 788–795.
[5] Orlowski, M., Michaud, C. and Chu, T.G. (1983) Eur. J. Biochem. 135, 81–88.
[6] Vincent, B., Jiracek, J., Noble, F., Loog, M., Roques, B., Dive, V., Vincent, J.-P. and Checler, F. (1997) Eur. J. Pharmacol. 334, 49–53.
[7] Barrett, A.J., Brown, M.A., Dando, P.M., Knight, C.G., McKie, N., Rawlings, N.D. and Serizawa, A. (1995) Methods Enzymol. 248, 529–556.
[8] Pierotti, A., Dong, K.W., Glucksman, M.J., Orlowski, M. and Roberts, J.L. (1994) Biochemistry 33, 622.
[9] Dauch, P., Vincent, J.-P. and Checler, F. (1995) J. Biol. Chem. 270, 27266–27271.
[10] Brown, C.K., Madauss, K., Lian, W., Beck, M.R., Tolbert, W.D. and Rodgers, D.W. (2001) Proc. Natl. Acad. Sci. USA 98, 3127–3132.
[11] Matthews, B.W. (1988) Acc. Chem. Res. 21, 333–340.
[12] Shrimpton, C.N., Glucksman, M.J., Lew, R.A., Tullai, J.W., Margulies, E.H., Roberts, J.L. and Smith, A.I. (1997) J. Biol. Chem. 272, 17395–17399.
[13] Gill, S.C. and Von Hippel, P.H. (1989) Anal. Biochem. 182, 319–326.
[14] Guex, N. and Peitsch, M.C. (1997) Electrophoresis 18, 2714–2723.
[15] Guex, N., Diemand, A. and Peitsch, M.C. (1999) Trends Biochem. Sci. 24, 364–367.
[16] Peitsch, M.C. (1995) Bio/Technology 13, 658–660.
[17] Wolfson, A.J., Shrimpton, C.N., Lew, R.A. and Smith, A.I. (1996) Biochem. Biophys. Res. Commun. 229, 341–348.
[18] Auld, D.S. and Vallee, B.L. (1970) Biochemistry 9, 4352–4359.
[19] Izquierdo-Martin, M. and Stein, R.L. (1992) J. Am. Chem. Soc. 114, 325–331.
[20] Kunugi, S., Hirohara, H. and Ise, N. (1982) Eur. J. Biochem. 124, 157–163.
[21] Mock, W.L. and Tsay, J.T. (1988) J. Biol. Chem. 263, 8635–8641.
[22] Ray, K., Hines, C.S. and Rodgers, D.W. (2002) Protein Sci. 11, 2237–2246.
[23] Holland, D.R., Hausrath, A.C., Juers, D. and Matthews, B.W. (1995) Protein Sci. 4, 1955–1965.
[24] Lipscomb, W.N. and Straeter, N. (1996) Chem. Rev. 96, 2375–2433.
[25] Arndt, J.W., Hao, B., Ramakrishnan, V., Cheng, T., Chan, S.I. and Chan, M.K. (2002) Structure 10, 215–224.
[26] Beaumont, A., O'Donohue, M.J., Paredes, N., Rousselet, N., Assicot, M., Bohuon, C., Fournie-Zaluski, M.-C. and Roques, B.P. (1995) J. Biol. Chem. 270, 16803–16808.
[27] Hausrath, A.C. and Matthews, B.W. (1994) J. Biol. Chem. 269, 18839–18842.
[28] Marie-Claire, C., Ruffet, E., Tiraboschi, G. and Fournie-Zaluski, M.-C. (1998) FEBS Lett. 438, 215–219.
[29] Yiallouros, I., Grose, E. and Stocker, W. (2000) FEBS Lett. 484, 224–228.
[30] Grams, F., Dive, V., Yiotakis, A., Yiallouros, I., Vassiliou, S., Zwilling, R., Bode, W. and Stocker, W. (1996) Nat. Struct. Biol. 3, 671–675.
[31] Oliviera, V., Araujo, M.C., Rioli, V., de Camargo, A.C.M., Terasario, I.L.S., Juliano, M.A., Juliano, L. and Ferro, E.S. (2003) FEBS Lett. 541, 89–92.